Title

In Silico Assessment of Efficacy and Safety of IKur Inhibitors in Chronic Atrial Fibrillation: Role of Kinetics and State-Dependence of Drug Binding.

Journal

Frontiers in pharmacology, 8(NOV)

ISSN

1663-9812

Authors

Ellinwood, Nicholas
Dobrev, Dobromir
Morotti, Stefano
et al.

Publication Date

2017

DOI

10.3389/fphar.2017.00799

Peer reviewed

frontiers in Pharmacology

ORIGINAL RESEARCH
published: 07 November 2017
doi: 10.3389/fphar.2017.00799

In Silico Assessment of Efficacy and Safety of I_{Kur} Inhibitors in Chronic Atrial Fibrillation: Role of Kinetics and State-Dependence of Drug Binding

Nicholas Ellinwood[1], *Dobromir Dobrev*[2], *Stefano Morotti*[1]* *and Eleonora Grandi*[1]

[1] *Department of Pharmacology, University of California, Davis, Davis, CA, United States,* [2] *West German Heart and Vascular Center, Institute of Pharmacology, University Duisburg-Essen, Essen, Germany*

Current pharmacological therapy against atrial fibrillation (AF), the most common cardiac arrhythmia, is limited by moderate efficacy and adverse side effects including ventricular proarrhythmia and organ toxicity. One way to circumvent the former is to target ion channels that are predominantly expressed in atria vs. ventricles, such as $K_V1.5$, carrying the ultra-rapid delayed-rectifier K^+ current (I_{Kur}). Recently, we used an *in silico* strategy to define optimal $K_V1.5$-targeting drug characteristics, including kinetics and state-dependent binding, that maximize AF-selectivity in human atrial cardiomyocytes in normal sinus rhythm (nSR). However, because of evidence for I_{Kur} being strongly diminished in long-standing persistent (chronic) AF (cAF), the therapeutic potential of drugs targeting I_{Kur} may be limited in cAF patients. Here, we sought to simulate the efficacy (and safety) of I_{Kur} inhibitors in cAF conditions. To this end, we utilized sensitivity analysis of our human atrial cardiomyocyte model to assess the importance of I_{Kur} for atrial cardiomyocyte electrophysiological properties, simulated hundreds of theoretical drugs to reveal those exhibiting anti-AF selectivity, and compared the results obtained in cAF with those in nSR. We found that despite being downregulated, I_{Kur} contributes more prominently to action potential (AP) and effective refractory period (ERP) duration in cAF vs. nSR, with ideal drugs improving atrial electrophysiology (e.g., ERP prolongation) more in cAF than in nSR. Notably, the trajectory of the AP during cAF is such that more I_{Kur} is available during the more depolarized plateau potential. Furthermore, I_{Kur} block in cAF has less cardiotoxic effects (e.g., AP duration not exceeding nSR values) and can increase Ca^{2+} transient amplitude thereby enhancing atrial contractility. We propose that *in silico* strategies such as that presented here should be combined with *in vitro* and *in vivo* assays to validate model predictions and facilitate the ongoing search for novel agents against AF.

Keywords: ultra-rapid delayed-rectifier K^+ current, atrial fibrillation, mathematical modeling, ion channel blockers

OPEN ACCESS

Edited by:
Domenico Tricarico, Università degli studi di Bari Aldo Moro, Italy

Reviewed by:
Adam Hill, Victor Chang Cardiac Research Institute, Australia
Clemens Möller, Hochschule Albstadt-Sigmaringen, Germany

***Correspondence:**
Stefano Morotti
smorotti@gmail.com

Specialty section:
This article was submitted to Pharmacology of Ion Channels and Channelopathies, a section of the journal Frontiers in Pharmacology

Received: *07 August 2017*
Accepted: *23 October 2017*
Published: *07 November 2017*

Citation:
Ellinwood N, Dobrev D, Morotti S and Grandi E (2017) In Silico Assessment of Efficacy and Safety of I_{Kur} Inhibitors in Chronic Atrial Fibrillation: Role of Kinetics and State-Dependence of Drug Binding. Front. Pharmacol. 8:799. doi: 10.3389/fphar.2017.00799

Abbreviations: AP, action potential; APD, AP duration; APD_{40}, APD to 40% repolarization; APD_{90}, APD to 90% repolarization; AF, atrial fibrillation; C, closed state; cAF, chronic AF; CaT, Ca^{2+} transient; CaT_{amp}, CaT amplitude; CL, cycle length; EAD, early afterdepolarization; E_m, membrane potential; ERP, effective refractory period; G_{Kur}, maximal conductance of the ultra-rapid delayed-rectifier K^+ current; I, inactivated state; I_{Kur}, ultra-rapid delayed-rectifier K^+ current; nSR, normal sinus rhythm; O, open state.

INTRODUCTION

Atrial fibrillation (AF) is characterized by rapid, irregular heart contractions following fast, disorganized electrical signals in the atria. AF is the most common cardiac arrhythmia, occurring in 1–2% of the general population and projected to increase dramatically in the coming decades (to 4% by 2050) with an aging westernized population (Andrade et al., 2014). The most effective current treatment for preventing recurrence of AF in the clinic is radiofrequency ablation. Pharmacological therapy against AF is limited by low efficacy and substantial adverse side effects including an increased risk of lethal ventricular tachyarrhythmias.

To maximize efficacy and minimize proarrhythmic risk, an AF-selective drug should exert potent effects on fibrillating atria without significantly impacting ventricular tissue function during normal sinus rhythm (nSR) (Ehrlich et al., 2008; Van Wagoner et al., 2015). A potential strategy to achieve this goal is to target ion channels that are predominantly expressed in atria vs. ventricles, such as $K_V1.5$, carrying the ultra-rapid delayed-rectifier K^+ current (I_{Kur}). Genetic mutations causing both loss- and gain-of-function of I_{Kur} have been associated with atrial arrhythmias in human (Olson et al., 2006; Christophersen et al., 2013; Colman et al., 2017). In a previous investigation, we used an *in silico* strategy to define optimal $K_V1.5$-targeting drug characteristics, including kinetics and state-dependent binding, that maximize AF-selectivity (i.e., fast pacing-rate selectivity) in human atrial cardiomyocytes (Ellinwood et al., 2017). Because this work was conducted in atrial cardiomyocytes under nSR conditions, the best-performing drug properties identified would have relevance for patients with paroxysmal AF that have not undergone extensive AF-related electrical remodeling (Grandi et al., 2012; Nattel and Dobrev, 2016).

Building on our previously established simulation framework, the major goal of this investigation was to determine the optimal drug characteristics of I_{Kur} inhibitors in long-standing persistent (chronic) AF (cAF) conditions. Although not a universal finding (Yue et al., 1997; Bosch et al., 1999; Grammer et al., 2000; Workman et al., 2001), previous reports showed that I_{Kur} is strongly diminished in cAF patients (Van Wagoner et al., 1997; Brandt et al., 2000; Van Wagoner and Nerbonne, 2000; Dobrev and Ravens, 2003; Christ et al., 2008; Caballero et al., 2010), making the therapeutic potential of inhibitors targeting this current uncertain (Ravens et al., 2013; Grandi and Maleckar, 2016). Indeed, evidence of anti-arrhythmic efficacy of $K_V1.5$ inhibitors in clinical trials is lacking (Ravens et al., 2013). However, recent studies have suggested an anti-arrhythmic potential of I_{Kur}-targeting drugs in cAF (Christ et al., 2008; Ford et al., 2013, 2016; Loose et al., 2014), as they can prolong action potential (AP) and effective refractory period (ERP) in atrial cardiomyocytes of cAF patients. Moreover, experimental evidence suggests that block of I_{Kur} enhances force of contraction of isolated human atrial trabeculae in cAF (Wettwer et al., 2004; Schotten et al., 2007). Our human atrial cardiomyocyte model confirmed that block of I_{Kur} results in prolongation and elevation of the AP plateau, which augments the Ca^{2+} transient (CaT) amplitude (CaT_{amp}), thereby eliciting a positive inotropic effect (Grandi et al., 2011). Thus, I_{Kur} might be a useful atrial-selective target to potentially prevent reentry and related atrial hypocontractility in cAF. We propose that our computational approach, combined with *in vivo* and *in vitro* validation, might be useful to facilitate the identification of atrial-selective anti-arrhythmic drugs against AF (Bers and Grandi, 2011; Grandi and Maleckar, 2016).

METHODS

Atrial AP Model and Simulations

APs and CaTs were simulated with the Grandi et al. model of the human atrial cardiomyocyte in nSR and cAF (Grandi et al., 2011; Morotti et al., 2016b). I_{Kur} gating was described by a 6-state Markov type model (**Figure 1A**) as in Ellinwood et al. (2017), and I_{Kur} maximal conductance (G_{Kur}) in cAF was reduced by 50% compared to nSR (Grandi et al., 2011).

Simulations were equilibrated for 300 beats at 1-Hz pacing or 900 beats at 3-Hz pacing. After the 300^{th} or 900^{th} beat, the time to 40 and 90% repolarization of the AP (APD_{40} and APD_{90}) were calculated, along with diastolic intracellular Ca^{2+} concentration ($[Ca^{2+}]_i$), CaT_{amp} and time to 50% CaT decay. The atrial ERP was determined using a standard S_1-S_2 premature stimulation protocol (Wang et al., 1996; Shinagawa et al., 2000; Christ et al., 2008; Zhao et al., 2009), where the S_1 basal stimulus (5 ms in duration) was applied to a steady-state human atrial cardiomyocyte model. As previously described (Ellinwood et al., 2017), ERP was determined by applying the premature S_2 stimulus (5 ms in duration, 2-fold the diastolic threshold of excitation) at progressively smaller S_1-S_2 intervals from 700 ms to refractoriness by decrements of 2 ms. The longest S_1-S_2 interval that failed to elicit an AP was taken as the local ERP (i.e., maximum upstroke velocity $\geq$5 V/s and AP with an amplitude $\geq$50% of the amplitude of the preceding AP elicited by S_1).

An irregular pacing protocol was run for 20 s, starting from steady-state conditions at the fixed 3-Hz pacing. The cycle length (CL) was allowed to vary randomly following a uniform distribution between 285.7 and 400 ms, corresponding to a minimum pacing frequency of 2.5 Hz and a maximum pacing frequency of 3.5 Hz, with a mean of 333.3 ms (corresponding to 3-Hz pacing). The time course of membrane potential (E_m), APD_{90}, and CL was tracked over the course of the simulation.

All simulations and analysis were performed in MATLAB (The MathWorks, Natick, MA, USA) using the stiff ordinary differential equation solver ode15s. The model code is available for download at the following webpages: https://somapp.ucdmc.ucdavis.edu/Pharmacology/bers/ and http://elegrandi.wixsite.com/grandilab/downloads.

Parameter Sensitivity Analysis

Parameter sensitivity analysis was performed with the population-based approach described in Sobie (2009), Morotti et al. (2017), and Morotti and Grandi (2017) to investigate the role of various currents and transporters in the regulation of AP duration (APD), ERP, and CaT characteristics. Two populations of 900 atrial cardiomyocyte models were generated by randomly

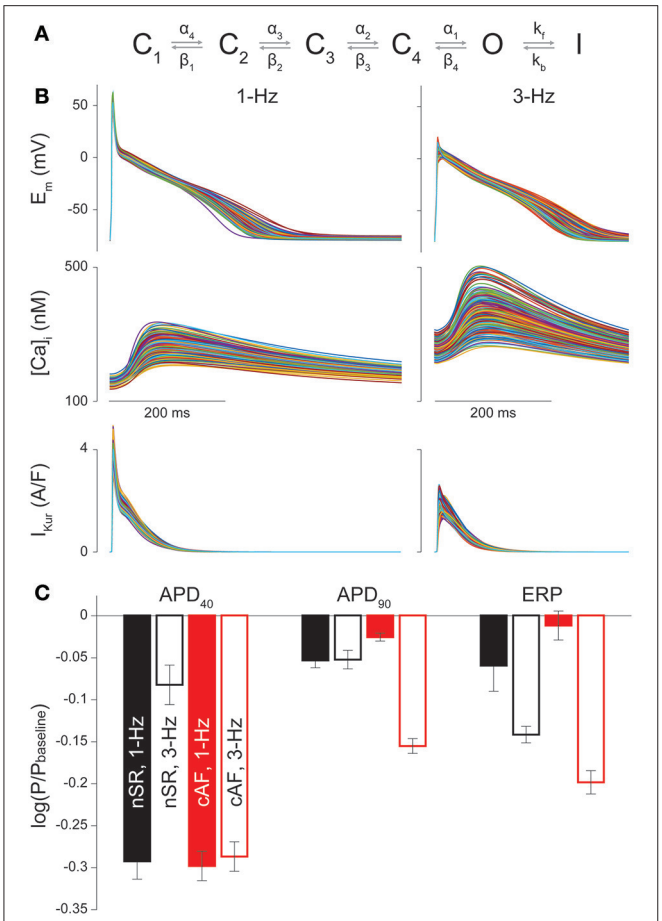

FIGURE 1 | Sensitivity of nSR and cAF cardiomyocyte electrophysiology to I_{Kur} changes. **(A)** Drug-free Markov model of I_{Kur} derived from Zhou et al. (2012). The model has 4 closed states (C_1, C_2, C_3, C_4), a conducting open state (O), and an inactivated state (I). Transition rates equations and parameters are those in Ellinwood et al. (2017). **(B)** AP, CaT, and I_{Kur} in a subset of 300 cAF cardiomyocyte model variants at 1-Hz and 3-Hz pacing rates. **(C)** Bar graphs show the average regression coefficients indicating how perturbations in G_{Kur} affect APD_{40}, APD_{90}, and ERP in nSR and cAF at 1-Hz and 3-Hz pacing rates. Error bars represent one standard deviation.

varying the values of 18 parameters (see list in the Supplementary Materials) in the baseline nSR and cAF models. Specifically, the default value of each conductance or maximal transport rate was independently varied with a log-normal distribution (with standard deviation of 0.1). Multivariable regression (non-linear iterative partial least squares method) on log-transformed values was performed for 30 random subsets of 300 model variants from the 900-variant population to correlate the variation in each parameter to the consequent effect on each output. In **Figure 1C** and Figures S1–S6 bars represent the mean regression coefficients and error bars represent one standard deviation.

K_V1.5 Drug-Binding Model

We utilized our recent I_{Kur} Markov formulation and approach to describe various drug-K_V1.5 channel binding schemes (**Figures 2A,F**; Ellinwood et al., 2017), as done by Lee et al. (2016). We previously showed that open state (O) blockers and open and inactivated state (O & I) blockers that target K_V1.5 display fast pacing-rate selectivity (Ellinwood et al., 2017). Thus, we focused on these two types of inhibitors when examining the relationship between electrophysiological parameters and drug-binding kinetics in cAF. We considered different theoretical drugs with variable forward (k_{on}) and reverse (k_{off}) drug-binding rates to the open and inactivated states of the K_V1.5 channel in the predicted physiological range of 0.01–100 s^{-1} (Lagrutta et al., 2006) using half-logarithmic increments resulting in nine transition rates for each drug state transition (0.01, 0.03, 0.1, 0.3, 1, 3, 10, 30, 100 s^{-1}). For a particular state of the channel, dissociation constants (K_d) for our drug scenarios were calculated as k_{off}/k_{on}, and affinity constants were calculated as k_{on}/k_{off}. To investigate the effects of these drug characteristics, for a given state-dependent binding inhibitor, we varied k_{on} and k_{off} together ($k_{on} = k_{off}$) or considered all permutations of the nine different rates of drug binding (producing a total of 81 different drug scenarios). For drugs that could bind to multiple states of the K_V1.5 channel, we also varied the relative affinity to open (K_O) vs. inactivated state (K_I). For O & I blockers, we included transitions between drug-bound states (orange transitions in **Figure 2F**) when specified. All drugs were simulated at the concentration causing a 50% reduction in peak I_{Kur} (i.e., IC_{50}). IC_{50} values were computed as described previously (Ellinwood et al., 2017), using a 200-ms down-ramp voltage-clamp protocol from +30 to −60 mV. After the application of a given [drug] (range: 1 nM−1 M), we allowed sufficient time for the degree of block to reach equilibrium. IC_{50} values were calculated at 1- and 3-Hz pacing rates as the [drug] causing a 50% reduction in peak I_{Kur} compared to drug-free conditions. We chose the down-ramp, as compared to a typical square pulse, because it more closely resembles the relative state occupancies of the closed states, open state, and inactivated state of the K_V1.5 channel during a physiological atrial AP, as we have shown in (Ellinwood et al., 2017).

RESULTS

Role of I_{Kur} in nSR and cAF Atrial Electrophysiology

We built 900 variations of our nSR and cAF human atrial cardiomyocyte models (Grandi et al., 2011) at 1- and 3-Hz pacing, and performed parameter sensitivity analysis on 30 random subsets of 300 model variants to determine how alterations in each maximum ionic conductance/transport rate differentially (in cAF vs. nSR) affect electrophysiological properties including APD_{40}, APD_{90}, ERP, CaT_{amp}, diastolic $[Ca^{2+}]_i$, and time to 50% CaT decay (Figures S1–S6). Simulated APs and CaTs in a representative group of 300 cAF cardiomyocyte model variants are shown in **Figure 1B**, and the average regression coefficients for G_{Kur} in nSR and cAF conditions at 1- and 3-Hz pacing are in **Figure 1C**. The values are negative because an increase in I_{Kur} shortens APD_{40}, APD_{90}, and ERP on average according to the regression algorithm. The analysis revealed that, while at a slow pacing rate APD_{90} and ERP

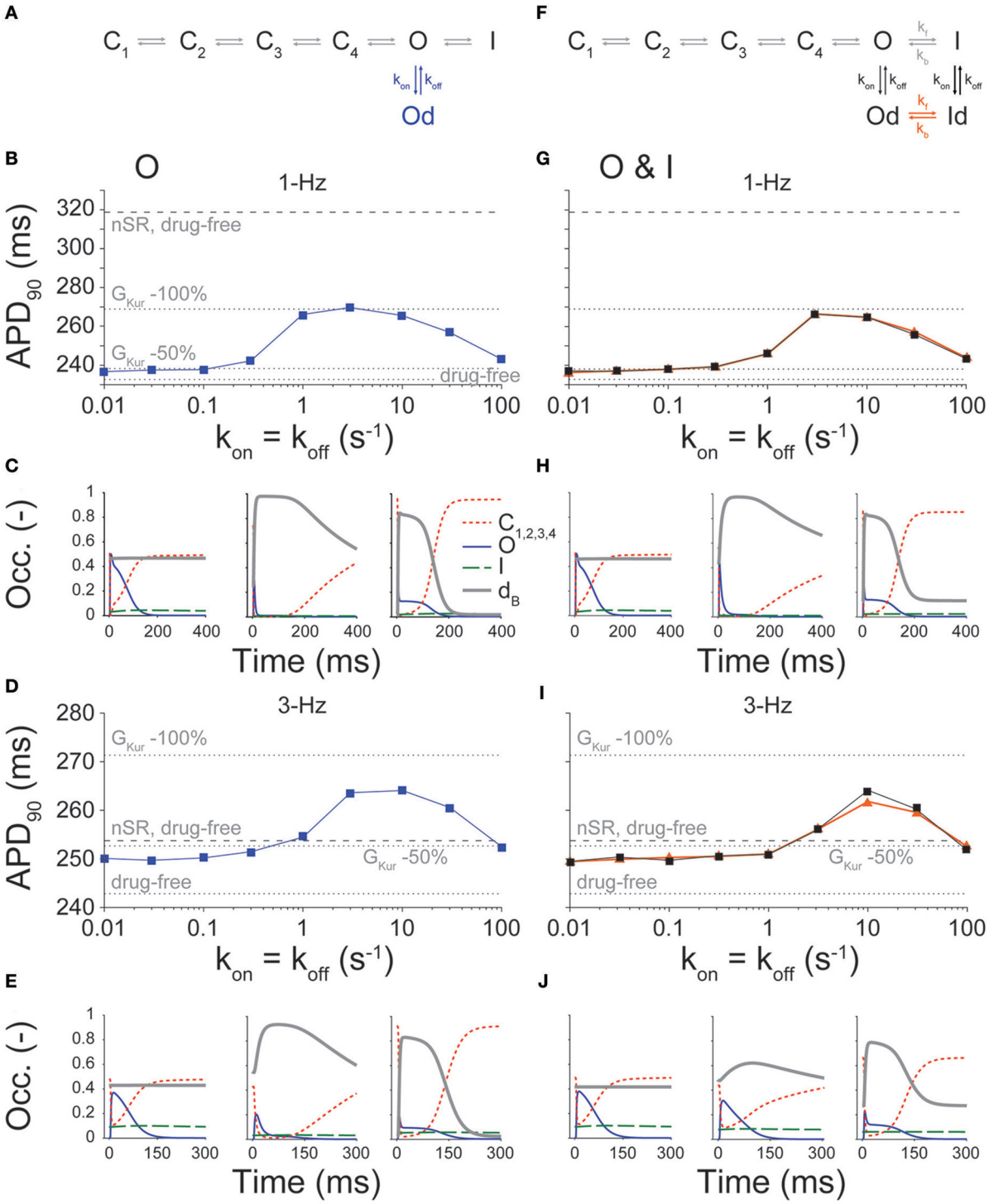

FIGURE 2 | Effect of state-dependence and kinetics of drug binding on APD_{90}. APD_{90} was determined for open (schematic in **A**, **B,** 1-Hz and **D**, 3-Hz pacing rate) and open and inactivated (schematic in **F**, **G** 1-Hz and **I**, 3-Hz pacing rate) state blockers given nine different rates of binding kinetics between 0.01 and 100 s^{-1} using half-logarithmic increments, whereby $k_{off} = k_{on}$, $K_d = 1\ \mu M$. For O & I blockers, we either allowed or prevented transitions between drug-bound states (orange vs. black traces in **G,I**). Simulations were also run in nSR and cAF drug-free conditions, and in cAF given a 50 and 100% reduction in G_{Kur} (dotted and dashed lines in **B**,**D**,**G**,**I**). Simulations were equilibrated for 300 beats at 1-Hz pacing or 900 beats at 3-Hz pacing using a [drug] equal to the IC_{50} value. **(C**,**E**,**H**,**J)** show the closed, open, inactivated and drug-bound (d_B, i.e., Od or Od+Id) state occupancies during an AP for three different drug-binding kinetics ($k_{off} = k_{on} = 0.01$, 3, and 100 s^{-1}).

are more sensitive to changes in G_{Kur}, APD_{40} is similarly sensitive in nSR and cAF (**Figure 1C**). At 3-Hz pacing, G_{Kur} impacts AP and ERP prolongation more in cAF vs. nSR despite the fact that G_{Kur} is smaller in cAF conditions. This points to I_{Kur} inhibition as a promising approach to counteract the abbreviated APD and ERP in cAF, while having a more moderate effect at physiological pacing rates. Therefore, we next ran simulations to reveal I_{Kur}-targeting drug properties that exhibit anti-AF selectivity and efficacy along with minimized proarrhythmic risk in cAF.

Effect of Conformational State Specificity and Binding/Unbinding Kinetics on Human Atrial Cardiomyocyte APD at Normal and Fast Pacing Rates in cAF Conditions

Figure 2 shows changes in APD caused by O and O & I inhibitors at varying drug-binding kinetics, whereby k_{on} is set equal to k_{off} (i.e., $K_d = 1\,\mu M$). These are compared to no block, 50, and 100% reduction in G_{Kur} in cAF conditions, as well as no block in nSR conditions. Similar to our findings in nSR (Ellinwood et al., 2017), both types of inhibitors display a biphasic relationship between APD and drug-binding kinetics at 1- and 3-Hz pacing. At 1-Hz pacing, APD in the presence of drug is comparable to a 50% reduction in G_{Kur} at slow and fast drug-binding kinetics (**Figures 2B,G**). Significant APD prolongation is only seen for intermediate drug-binding kinetics (0.3–30 s^{-1} for the open state blocker and 1–30 s^{-1} for the open and inactivated state blocker), and goes well beyond the little APD prolongation resulting from a constant 50% reduction in G_{Kur}. However, even the maximal APD prolongation produced by an O or O & I inhibitor in cAF is still ∼50 ms less than the APD in nSR in drug-free conditions, which we interpret to suggest that such drugs would have limited toxicity at 1-Hz pacing rate.

At 3-Hz pacing, the two types of inhibitors cause stronger relative prolongation as compared to 1-Hz pacing across the same range of drug-binding kinetics (**Figures 2D,I**). Notably, all simulated drugs caused APD prolongation at 3-Hz pacing, but the maximal prolongation produced by these theoretical inhibitors did not match the APD prolongation caused by a 100% reduction in G_{Kur}. However, drugs with intermediate drug-binding kinetics (3–30 s^{-1} for the O blocker and 10–30 s^{-1} for the O & I blocker) did extend the APD at 3-Hz pacing above the APD in nSR conditions given no block of I_{Kur}. Thus, even though G_{Kur} is reduced by 50% in cAF as compared to nSR, **Figure 2** illustrates that I_{Kur} inhibitors can still prolong APD in cAF, particularly at 3-Hz pacing.

Figures 2C,H,E,J display the closed (red), open (blue), inactivated (green), and drug-bound (gray) state occupancies during the steady-state AP for the slowest (0.01 s^{-1}), intermediate (3 s^{-1}), and fastest (100 s^{-1}) drug-binding rates. In general, for the slowest drug-binding kinetics, the inhibitors do not bind readily during the AP, and the drug-bound state stays level below 0.4. At intermediate drug-binding kinetics, the inhibitors bind readily during the AP, thus significantly shrinking the open state occupancy. In addition, the off-rate of drug binding is slow enough to achieve maintenance in the drug-bound state during the AP. This allows for considerable AP prolongation, almost mimicking complete block of I_{Kur}. Finally, for the fastest drug-binding kinetics, the drugs again bind readily during the AP, but the off-rate of drug binding is so fast as to cause cycling between the drug-free open state and the drug-bound open state during a single AP. This results in prolongation of the drug-free open state occupancy later in the AP that limits AP prolongation. These results are consistent with our previous simulations in nSR. However, given the more positive plateau in the cAF cardiomyocyte AP, $K_V1.5$ channels stay open longer, and inactivate more markedly (especially at 3-Hz pacing) as compared to nSR (Figure S7).

Given not only the rapid, but irregular electrical activity seen with AF, we sought to determine how the kinetics of drug binding of I_{Kur} inhibitors affected the time course of E_m (**Figure 3B**) and APD_{90} (**Figure 3C**) in cAF cardiomyocytes with a randomly variable CL (**Figure 3A**). Results in drug-free conditions and for an O & I blocker (modeled as in **Figure 2F**, black) with $k_{on} = k_{off}$ ($K_d = 1\,\mu M$) in **Figure 3** again demonstrate a biphasic relationship between drug-binding kinetics and average APD_{90} (**Figure 3D**), as seen with constant pacing (**Figure 2I**). Thus, for all future simulations, we used a constant pacing interval that can more easily be standardized in a high-throughput drug-screening process.

Effect of Conformational State Specificity and Binding/Unbinding Kinetics on Human Atrial Cardiomyocyte ERP at Normal and Fast Pacing Rates in cAF Conditions

The desired effect of I_{Kur} inhibitors is prolongation of atrial ERP (Amos et al., 1996; Christ et al., 2008; Sanchez et al., 2012; Loose et al., 2014; Ford et al., 2016), particularly during fast pacing rates typifying AF. Thus, we assessed the effects of binding/unbinding kinetics on the ERP for O (**Figures 4A,B**) and O & I (**Figures 4C,D**) blockers. Simulations reveal a similar biphasic relationship between ERP and drug-binding kinetics at 1- and 3-Hz pacing for both types of inhibitors, which mirror the drugs' effects on APD (**Figure 2**).

At 1-Hz pacing, I_{Kur} inhibitors cause minimal ERP prolongation at slow drug-binding rates (≤0.3 s^{-1} for O blockers and ≤1 s^{-1} for O & I blockers) and fast drug-binding rates (100 s^{-1}). Although substantial ERP changes are predicted at intermediate drug-binding rates (1–30 s^{-1} for O blockers and 3–30 s^{-1} for O & I blockers), ERP prolongation remains ∼62 ms lower than the ERP in nSR given no block of I_{Kur} for both inhibitors.

At 3-Hz pacing, however, I_{Kur} inhibitors appear to be more effective at extending ERP than APD, which is a favorable drug property as previously demonstrated for Class I antiarrhythmic drugs which cause clinically relevant post-repolarization refractoriness. For all drug-binding kinetics, ERP prolongation is at least equivalent to that caused by a constant 50% reduction in G_{Kur} (**Figures 4B,D**). Notably, for intermediate drug-binding kinetics (3–30 s^{-1} for O inhibitors and 10–30 s^{-1} for O & I inhibitors), drug-induced ERP prolongation extends above the ERP in nSR in drug-free conditions, and the fastest drug-binding kinetics prolong the ERP to a point that closely

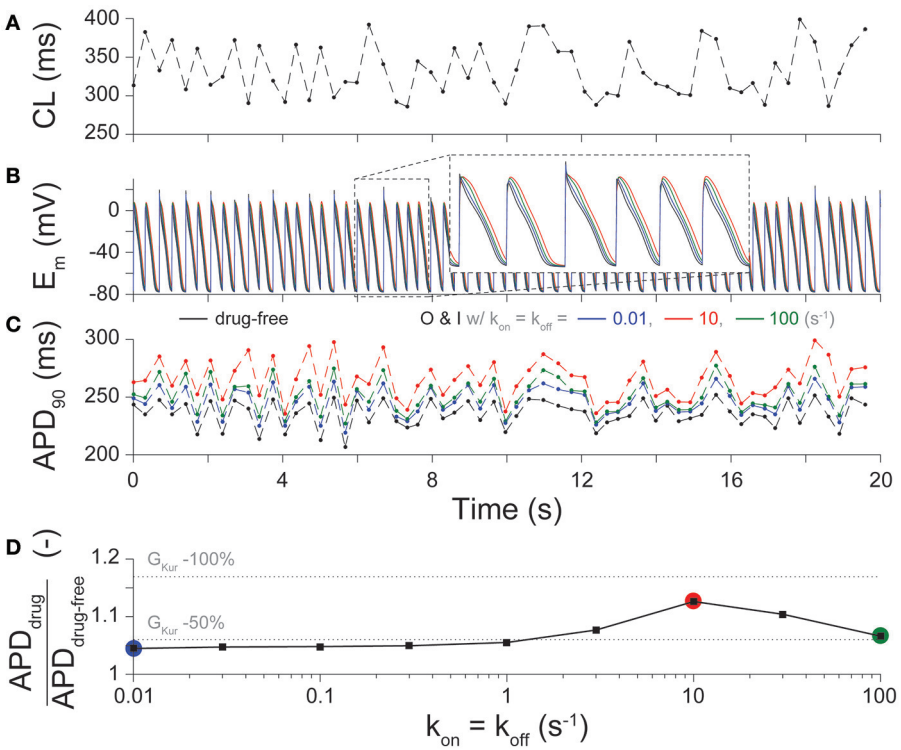

FIGURE 3 | Effect of drug-binding kinetics on APD during irregular pacing**. (A)** Beat-to-beat changes in CL during a 20-s irregular pacing protocol and the resultant time-course of **(B)** E_m, and **(C)** APD_{90} are shown in cAF cardiomyocytes in drug-free conditions (black), and for O & I blockers with slow (0.01 s^{-1}, blue), intermediate (10 s^{-1}, red), and fast (100 s^{-1}, green) drug-binding kinetics, given $k_{on} = k_{off}$. **(D)** summarizes the percent prolongation (mean APD_{90} after application of drug divided by mean APD_{90} in drug-free conditions during the simulation) for nine different rates of binding kinetics between 0.01 and 100 s^{-1} using half-logarithmic increments, whereby $k_{on} = k_{off}$, $K_d = 1\,\mu M$. These results are compared to 50, and 100% reduction in G_{Kur} (dotted lines) given the same irregular pacing protocol in **(A)**.

resembles that in nSR in drug-free conditions. These drugs showing substantial ERP prolongation at 3-Hz pacing in cAF (with APD at slow pacing rates being well below that in nSR, see **Figure 2**) might represent suitable compounds for AF-selective therapy.

Effects of Drug Binding/Unbinding Kinetics with Variable K_d on APD, ERP, and Ca^{2+} Handling

Figures 2, **3**, **4** show the results from drug scenarios where the on- and off-rate of drug binding are equal to one another ($k_{on} = k_{off}$, $K_d = 1\,\mu M$), but even closely related I_{Kur} inhibitors can have dissimilar K_d values (Lagrutta et al., 2006). Thus, we simulated all permutations of the nine different rates of drug binding (0.01 to 100 s^{-1}), yielding 81 different combinations of k_{on} and k_{off} for the O & I state inhibitors (assuming equal affinities for open and inactivated states) at 1- and 3-Hz pacing. We assessed the effects of these drugs (at their IC_{50} concentration) on APD, ERP, CaT_{amp}, and diastolic $[Ca^{2+}]_i$. **Figure 5** shows the output of the simulations for an O & I inhibitor (modeled as in **Figure 2F**, black) in the form of a heatmap, where the diagonals of the squares from the bottom left to the top right corner correspond to drug scenarios where $k_{on} = k_{off}$ ($K_d = 1\,\mu M$). Except for the drugs with the largest K_d values ($k_{off} >> k_{on}$), when k_{on} is held constant, APD, ERP, and Ca^{2+} handling are not very sensitive to changes in k_{off}. Thus, the effects of I_{Kur} inhibitors on atrial electrophysiology and Ca^{2+} handling are largely driven by k_{on} rates as compared to k_{off} rates.

In cAF conditions, ideal I_{Kur} inhibitors exhibiting AF-selectivity will prolong atrial refractoriness (ERP prolongation at 3-Hz pacing), have limited toxicity (minimal to no APD prolongation at 1-Hz pacing), and have a positive inotropic effect (an increase in CaT_{amp} at 1-Hz pacing). O & I inhibitors with a large K_d do not display any of the desired favorable drug properties including prolongation of ERP at 3-Hz pacing (**Figure 5B**) or increase in CaT_{amp} (**Figures 5C,D**), as their effects on APD, ERP, and Ca^{2+} handling are minimal, resembling drug-free conditions. Intermediate k_{on} rates (3–30 s^{-1} for 1-Hz pacing and 10–30 s^{-1} for 3-Hz pacing) cause the most significant increase in all the outputs displayed in **Figure 5**. For example, drugs with a k_{on} rate equal to 10 s^{-1} cause the greatest ERP prolongation at 3-Hz pacing (**Figure 5B**) and increase in CaT_{amp} and diastolic $[Ca^{2+}]_i$ (**Figures 5C,E**). Note, there is also significant APD prolongation at 1-Hz pacing when k_{on} is in the intermediate drug-binding range (**Figure 5A**), but none of the 81 permutations of the simulated open and inactivated state inhibitor cause the APD to get close to the APD in nSR at 1-Hz

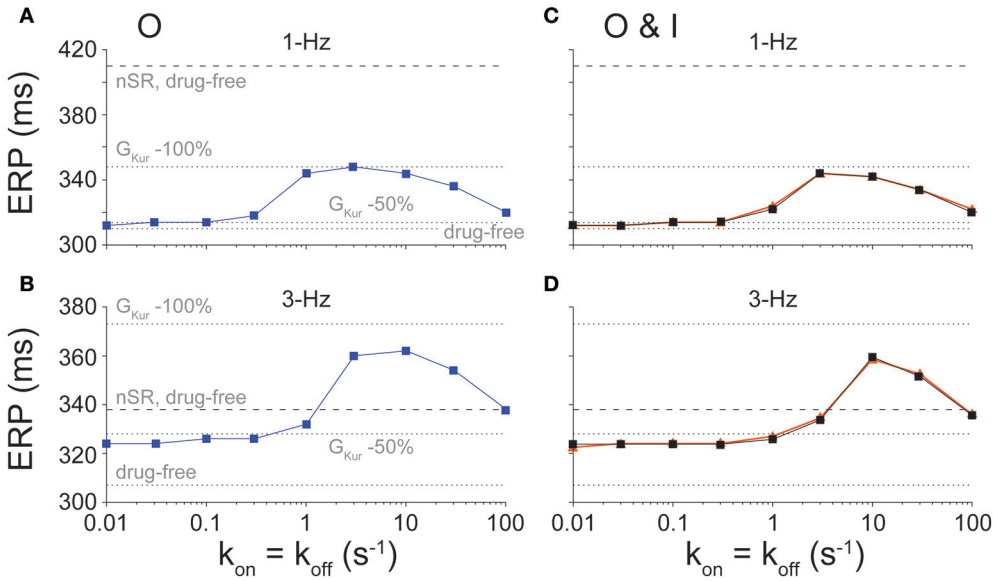

FIGURE 4 | Effect of state-dependence and kinetics of drug binding on ERP. ERP was determined for open (**A**, 1-Hz and **B**, 3-Hz pacing rate) and open and inactivated (**C**, 1-Hz and **D**, 3-Hz pacing rate) state blockers given nine different rates of binding kinetics between 0.01 and 100 s^{-1} using half-logarithmic increments, whereby $k_{off} = k_{on}$, $K_d = 1\,\mu M$. For O & I blockers, we either allowed or prevented transitions between drug-bound states (orange vs. black traces in **C,D**). Simulations were also run in nSR and cAF drug-free conditions, and in cAF given a 50 and 100% reduction in G_{Kur}.

pacing (320 ms). Thus, the APD prolongation seen in **Figure 5A** does not necessarily disqualify any of these theoretical drug candidates for AF therapy. Likewise, at 3-Hz pacing, the increase in CaT_{amp} and diastolic $[Ca^{2+}]_i$ mirrors the prolongation in APD and ERP at 3-Hz pacing (**Figures 5D,F**). While an excessive increase in diastolic $[Ca^{2+}]_i$ might be deleterious, we find it to remain well below the predicted value in the nSR human atrial cardiomyocyte model (~360 nM).

In our previous study in nSR (Ellinwood et al., 2017), we found that O & I inhibitors with the fastest drug-binding kinetics (30–100 s^{-1}) cause ERP prolongation at 3-Hz pacing and no APD prolongation at 1-Hz pacing. These same inhibitors display favorable fast pacing-rate selectivity in atrial cardiomyocytes from cAF according to our simulations shown in **Figures 5A,B**. However, if we are not as concerned with APD prolongation in cAF conditions at 1-Hz pacing, then drugs with a k_{on} rate in the intermediate drug-binding range (3–30 s^{-1}) would also be efficacious and perhaps more efficacious since they cause a positive inotropic effect at 1-Hz pacing (**Figures 5C,E**).

Effect of Relative State-Specific Drug Binding

Because many I_{Kur} inhibitors bind to multiple states of $K_V1.5$ with variable affinity (Bouchard and Fedida, 1995; Lagrutta et al., 2006; Ford et al., 2016), we allowed k_{on} for the open state ($k_{on,O}$), k_{off} for the open state ($k_{off,O}$), k_{on} for the inactivated state ($k_{on,I}$), and k_{off} for the inactivated state ($k_{off,I}$) to have any of the three binding rates (0.01, 3, and 100 s^{-1}), and varied them independently to yield 81 different drug combinations. We studied the effects of these I_{Kur} blockers in cAF conditions using a [drug] equal to their IC_{50} value at 1-Hz pacing for APD and 3-Hz pacing for ERP. Then, we compared the outputs of APD and ERP to no block, 50, and 100% reduction in G_{Kur} in cAF conditions (**Figure 6**, dotted lines), along with no block in nSR conditions (**Figure 6**, dashed lines).

Figures 6A,B display the relationship between APD (at 1-Hz pacing) and K_O/K_I. Data points in **Figure 6A** are separated by IC_{50} cutoffs of 0.1 μM, 10 μM, and 1 mM, and show that when $K_O/K_I < 1$, we almost always obtain maximal AP prolongation (this also corresponds to larger IC_{50} values). In **Figure 6B**, we separated the points according to the drug's $k_{off,O}$ rate (0.01, 3, or 100 s^{-1}), which revealed that when $K_O/K_I > 1$, we only obtain significant AP prolongation when $k_{off,O}$ is equal to 3 s^{-1} (i.e., the intermediate drug-binding rate). These results in the cAF-remodeled atrial cardiomyocyte correspond well with the results from our previous study of I_{Kur} inhibitors in nSR (Ellinwood et al., 2017). Nevertheless, none of the 81 simulated O & I inhibitors in **Figure 6** prolong the AP beyond the APD found in nSR at 1-Hz pacing.

Figures 6C,D present the relationship between APD at 1-Hz pacing and ERP at 3-Hz pacing for the O & I inhibitors with a variable K_O/K_I ratio. In **Figure 6C**, light gray symbols correspond to $K_O/K_I \leq 1$, and dark symbols correspond to $K_O/K_I > 1$). The O & I blockers displaying favorable pacing-rate selectivity, i.e., producing ERP prolongation at 3-Hz pacing while having moderate effect on APD (and ERP) at 1-Hz pacing, are the ones with $K_O/K_I > 1$, except if $k_{off,O}$ equals 3 s^{-1}. However, as none of the 81 simulated O & I inhibitors in **Figure 6** prolong the APD beyond that found in nSR at 1-Hz pacing, one could argue that none of the drugs is expected to cause harmful AP prolongation when AF is terminated. To try and enrich our metric, in **Figure 6D** we also categorize the drugs according to

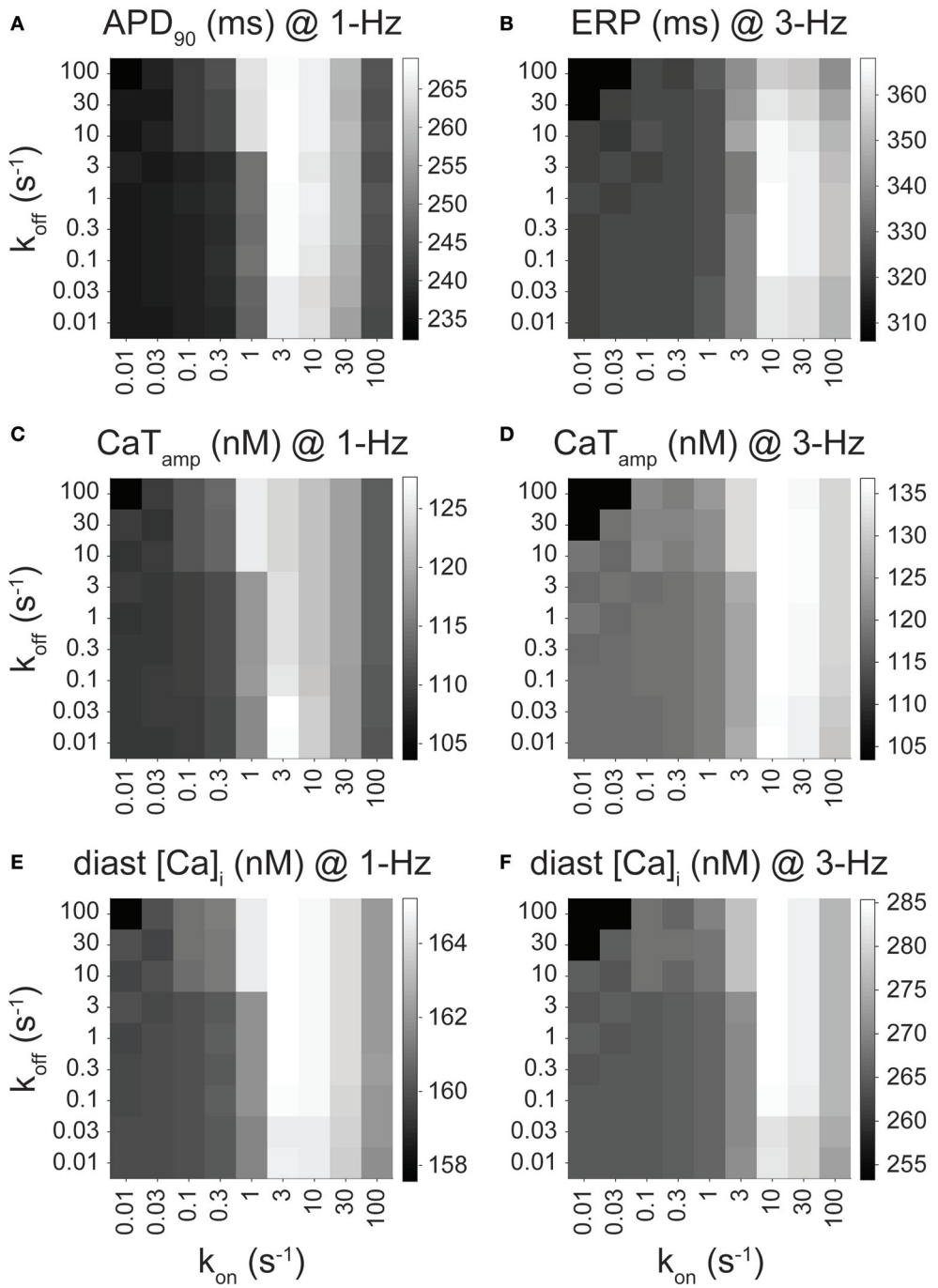

FIGURE 5 | Effect of drug-binding kinetics on APD_{90}, ERP, CaT_{amp}, and diastolic $[Ca^{2+}]_i$ for an open and inactivated state blocker. **(A)** APD_{90} (at 1 Hz), **(B)** ERP (at 3 Hz), **(C,D)** CaT_{amp} (at 1 and 3 Hz), and **(E,F)** diastolic $[Ca^{2+}]_i$ (at 1 and 3 Hz) are plotted for open and inactivated state blockers with varying binding kinetics, which were simulated via permutations of nine different drug-binding rates of (from 0.01 to 100 s^{-1}) while keeping $k_{on,O} = k_{on,I}$ and $k_{off,O} = k_{off,I}$. CaT_{amp} is 103.6, 109.4, and 120.4 nM at 1 Hz, and 103.4, 120.4, and 135.9 nM at 3 Hz for drug-free, 50 and 100% I_{Kur} block, respectively. Diastolic $[Ca^{2+}]_i$ is 157.6, 160.0, and 165.2 nM at 1 Hz, and 253.3, 266.9, and 286.9 nM at 3 Hz for drug-free, 50 and 100% I_{Kur} block, respectively.

percent increase in CaT_{amp}. The best-performing drugs will cause ERP prolongation at 3-Hz pacing in cAF (above nSR), and have a positive inotropic effect (**Figure 6D**, black). Corresponding with the results showcased in **Figure 5**, drugs with intermediate binding rates (e.g., $k_{off,O} = 3\ s^{-1}$) may thus be favorable given their stronger inotropic effect.

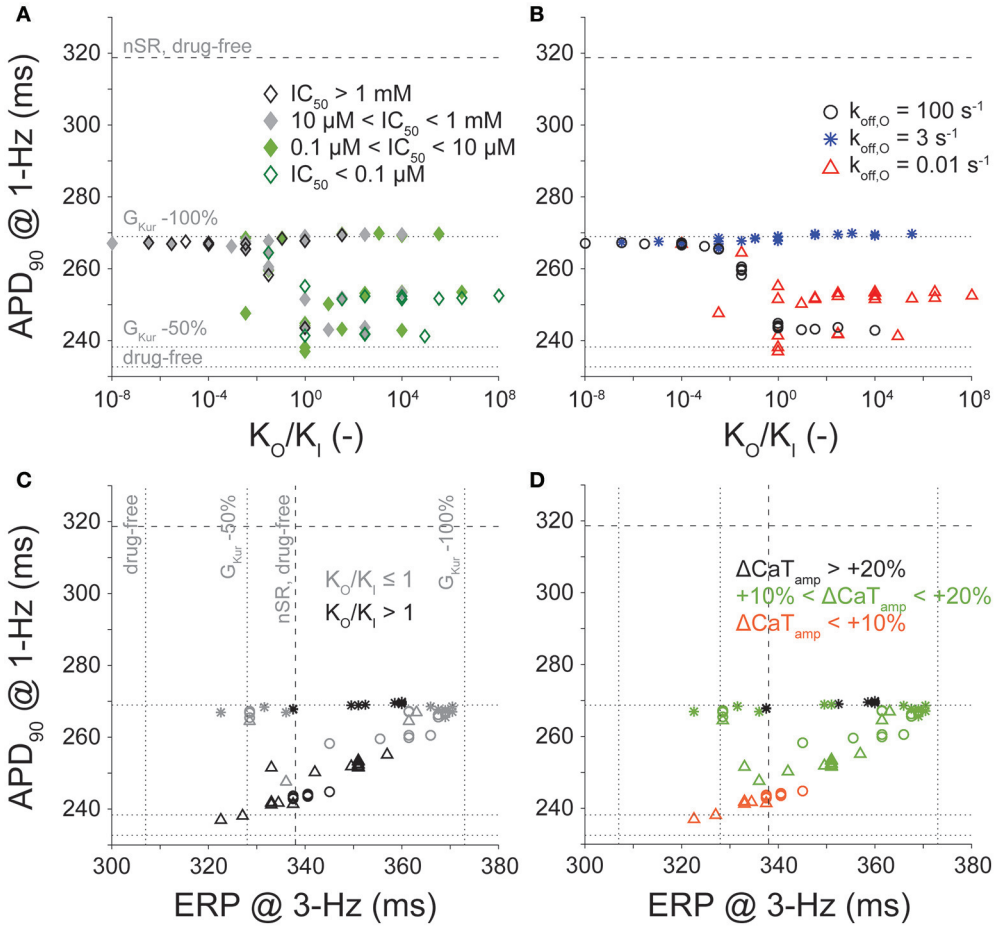

FIGURE 6 | Effect of conformational state affinity and drug-binding kinetics of an open and inactivated state blocker on APD_{90}, ERP, and Ca^{2+} handling. Open and inactivated state I_{Kur} blockers with varying affinities to the open and inactivated states were simulated via permutations of three different rates of binding kinetics (0.01, 3, and 100 s^{-1}). Simulations were equilibrated for 300 beats at 1-Hz pacing or 900 beats at 3-Hz pacing using a [drug] equal to the IC_{50} value. **(A,B)** report APD_{90} values (at 1 Hz) plotted as a function of the ratio of the open to the inactivated state affinity (K_O/K_I) used in each simulation. **(C,D)** report APD_{90} (at 1 Hz) and ERP values (at 3 Hz). Color code in **(A)** is for IC_{50} levels. Symbols in **(B,C,D)** indicate various $k_{off,O}$. Shades in **(C)** reflect either higher affinity to the open or the inactivated state. Color code in **(D)** corresponds to the variable degree of CaT_{amp} increase (at 1 Hz) induced by I_{Kur} block. Horizontal and vertical lines represent APD_{90} and ERP values obtained in cAF in drug-free conditions, and 50 and 100% reduction in G_{Kur} (dotted lines), and in nSR in drug-free conditions (dashed lines).

DISCUSSION

In this study, we sought to determine if I_{Kur} is a suitable anti-AF target despite it being downregulated in cAF patients, and, if so, what are the kinetic and state-dependent binding properties that maximize anti-AF efficacy and limit potential cardiotoxicity. Building off our previous study in nSR conditions (Ellinwood et al., 2017), we implemented an *in silico* assessment of I_{Kur} inhibitors in cAF atrial cardiomyocyte models, and identified metrics for delineating ideal $K_V1.5$ blockers against AF. Our results point to I_{Kur} inhibition as a valid strategy to prolong atrial refractoriness also generating a positive inotropic effect in cAF conditions. Although increasing force generation may not be a useful therapeutic goal at the high atrial rates seen during AF, it can be important to counteract atrial hypocontractility after cardioversion of AF to nSR. Interestingly, our simulations suggest that electrophysiological properties in cAF cardiomyocytes, such as shorter AP and more depolarized plateau potential, both might act to increase efficacy and dampen cardiotoxicity of potential $K_V1.5$-targeting drugs as compared to nSR (Ellinwood et al., 2017; **Figure 7**).

I_{Kur} Role in APD and ERP Regulation Is Preserved Despite Its Downregulation in cAF

Figure S7 shows the differences in the time courses of E_m, I_{Kur}, and closed, open, and inactivated state occupancies of $K_V1.5$ in cAF and nSR during the AP. Despite the reduced peak current, the channel stays open later in cAF (at both 1- and 3-Hz pacing) because of the more depolarized AP plateau. Thus, the consequences of I_{Kur} inhibition, including the extent of AP

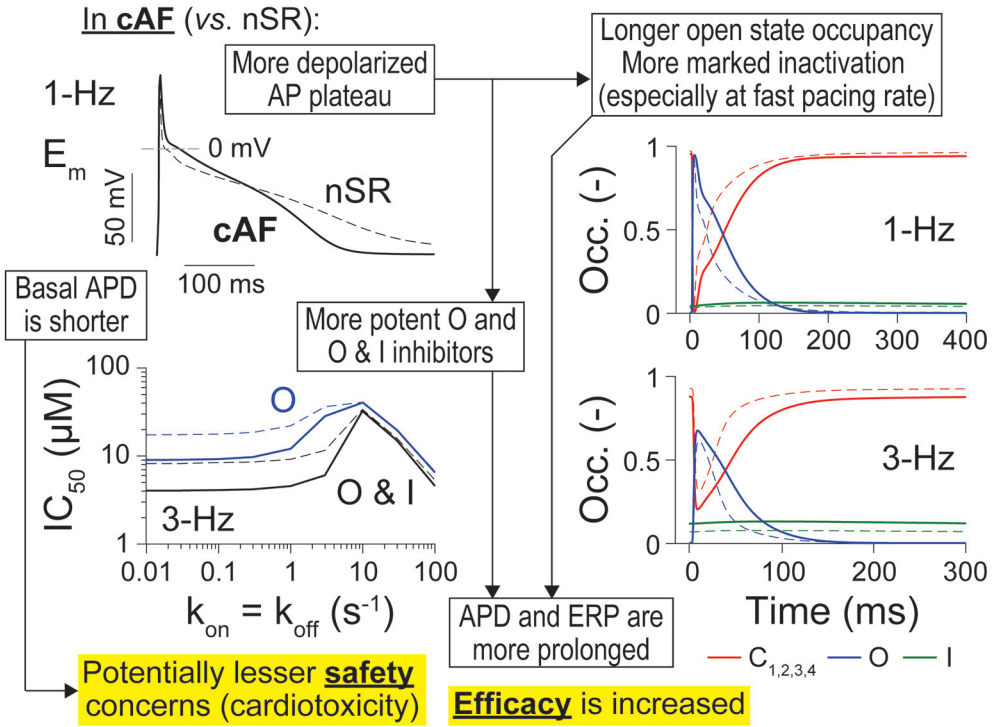

FIGURE 7 | Summary of main findings. Atrial cardiomyocytes in cAF (solid lines) vs. nSR (dotted lines) have different AP trajectories, including a shorter APD and more depolarized plateau (top left). The latter causes longer open state occupancy (right, blue solid vs. dashed lines) and stronger inactivation of the channel in cAF conditions (especially at fast pacing rates, right, green solid vs. dashed lines). I_{Kur} inhibitors appear also more potent in cAF vs. nSR (bottom left). These factors render APD and ERP more sensitive to inhibition by O and O & I inhibitors of $K_V1.5$, thus increasing efficacy of these drugs in cAF vs. nSR. Because basal APD is shorter in cAF, there are potentially less safety concerns due to drug-induced AP prolongation and subsequent afterdepolarization-driven proarrhythmia.

and ERP prolongation, depend not only on I_{Kur} magnitude (i.e., maximal conductance), but also on other fluxes affected by AF-induced remodeling, which affect E_m and thus E_m-dependent properties of I_{Kur} (**Figure 7**). For example, our group and others have hypothesized that the extent of AP and ERP prolongation due to I_{Kur} blockade depends on the AF-induced remodeling of other K^+ currents (Lagrutta et al., 2006; Morotti et al., 2016a; Aguilar et al., 2017; Colman et al., 2017), and relative strengths of I_{CaL} and I_{Kur} (Wettwer et al., 2004; Grandi and Maleckar, 2016). Our sensitivity analysis (**Figure 1C** and Figures S1–S6) revealed that APD_{90} and ERP are more sensitive to changes in G_{Kur} at fast vs. slow pacing rates. Aguilar et al. recently determined that the relative contribution of I_{Kur} to AP repolarization increases at higher frequencies because of reduced activation of the rapid delayed-rectifier current I_{Kr} (Aguilar et al., 2017). Our results concur with these findings, as our sensitivity analysis shows that APD_{90} and ERP are less sensitive to changes in G_{Kr} at 3-Hz pacing as compared to 1-Hz pacing in nSR conditions (Figures S2, S3). Most importantly, we also found that G_{Kur} impacted the duration of AP repolarization and refractoriness more in cAF vs. nSR (even though this parameter was halved in the cAF model) at 3-Hz, but not at 1-Hz pacing (i.e., fast pacing-rate selectivity). This is a favorable drug property to avoid harmful AP prolongation (which is also limited by the reduced basal APD) if AF is terminated. Similar to Aguilar et al. (2017), our results suggest that the APD- (and ERP)-prolonging effect of I_{Kur} block is not affected by I_{Kur} downregulation.

Enhanced Efficacy and Safety of I_{Kur} Inhibitors in cAF vs. nSR

We focused here on O and O & I blockers because we have previously shown that these inhibitors display fast pacing-rate selectivity in nSR (Ellinwood et al., 2017). This choice was also supported by the increased occupancy of open and inactivated states in cAF conditions (**Figure 7**). In our previous report in nSR (Ellinwood et al., 2017), we found that when $k_{on} = k_{off}$ (i) slow drug-binding kinetics caused minimal APD changes and modest ERP prolongation; (ii) intermediate drug-binding kinetics led to substantial AP and ERP prolongation; and (iii) fast drug-binding kinetics failed to produce substantial AP or ERP prolongation at normal pacing rate, but increased the ERP at 3-Hz pacing. While in cAF the overall biphasic relationship between APD/ERP and drug-binding kinetics was maintained (see **Figures 2–4**), notably, at 1-Hz pacing rate, even the maximal AP prolongation induced by I_{Kur} inhibition in cAF is not sufficient to reach the APD observed in nSR in drug-free conditions. This might indicate that there are less safety concerns for $K_V1.5$ block in cAF patients. At 3-Hz pacing, ERP prolongation is at least equivalent to that caused by a constant 50% reduction in G_{Kur}, and, for intermediate and fast drug-binding kinetics, the ERP

is equal to or greater than the one obtained in nSR in drug-free conditions. These observations suggest that O and O & I inhibitors have a broader range of efficacy in cAF vs. nSR. We assessed whether closed state inhibitors, which displayed reverse-rate dependence in terms of potency (Ellinwood et al., 2017), may also be effective and safe anti-AF agents in cAF conditions (Figure S8). We found that these blockers prolong ERP at 3-Hz pacing (Figure S8G) while minimally prolonging the cAF AP at 1-Hz pacing at the fastest drug-binding kinetics ($\geq$30 s^{-1}, Figure S8B). However, they had a smaller maximal effect and kinetic range for prolonging the ERP at 3-Hz pacing beyond nSR conditions as compared to O and O & I blockers.

We enriched our metric for quantifying anti-AF efficacy and safety of I_{Kur} inhibitors by also accounting for changes in Ca^{2+}-handling parameters, namely CaT_{amp} and diastolic $[Ca^{2+}]_i$ (Tsujimae et al., 2008; Cavero and Holzgrefe, 2014; Lancaster and Sobie, 2016; Li et al., 2017), which provided additional detail to refine the search for best-performing drugs. In identifying the ideal drug characteristics, we looked for inhibitors that prolong ERP (especially at fast pacing rates), limit APD prolongation at slow pacing-rates, and improve atrial inotropy, i.e., increase CaT_{amp}. Increasing force generation might be a useful outcome after cardioversion to nSR.

When $K_O = K_I$, the best-performing O & I inhibitors were those with intermediate k_{on} rates (3–30 s^{-1}), because they prolonged ERP at 3-Hz pacing and increased CaT_{amp} and diastolic $[Ca^{2+}]_i$ at 1-Hz pacing (**Figure 5**). These inhibitors also prolonged the AP at 1-Hz pacing and increased CaT_{amp} and diastolic $[Ca^{2+}]_i$ at 3-Hz pacing—thus potentially predisposing to harmful AP prolongation and Ca^{2+} overload. However, we note that such cardiotoxicity is unlikely considering the fact that the maximum increases of APD and CaT_{amp} still remain far below the corresponding values obtained in nSR in drug-free conditions. In our previous study, we highlighted that the best-performing drugs in nSR were the O & I inhibitors with the fastest drug-binding kinetics (Ellinwood et al., 2017). While these drugs are still efficacious at prolonging ERP at 3-Hz pacing in cAF, they have limited effect on Ca^{2+} handling.

When K_I and K_O were varied, the relationships between APD at 1-Hz pacing and affinity ratio (K_O/K_I) are similar to those in nSR (**Figures 6A,B**; Ellinwood et al., 2017), except none of the 81 simulated O & I inhibitors prolonged the AP beyond the duration found in nSR in drug-free condition. Likewise, the relationship between APD at 1-Hz pacing and ERP at 3-Hz pacing is similar to nSR (**Figures 6C,D**; Ellinwood et al., 2017), but none of the drugs exhibit obvious toxicity. The same O & I inhibitors simulated in cAF conditions were more effective at prolonging ERP at 3-Hz pacing rates as compared to nSR conditions. Thus, on average, the same inhibitors in **Figure 6** exhibit less toxicity and greater efficacy in cAF vs. nSR.

In their simulation study, Aguilar et al. concluded that the ability of (simple pore) I_{Kur} block to terminate simulated AF was greatly attenuated by remodeling, because the block-induced AP prolongation was insufficient to counteract the strong effects of cAF-induced remodeling (Aguilar et al., 2017). Notably, here we show that depending on the drug-binding kinetics, certain I_{Kur} inhibitors can markedly counteract the effect of cAF-associated remodeling, and bring AP and ERP parameters close to nSR values, i.e., have a greater effect than simple pore blockers.

Limitations and Future Directions

We presented a theoretical study of the effects of I_{Kur} inhibitors in cAF, and compared our results to our previous study in nSR atrial cardiomyocytes. We acknowledge several limitations to the described approach, which provide opportunities for further extensions. First, we only considered direct drug effects on $K_V1.5$, and future analysis should consider multi-channel effects of I_{Kur} inhibitors (Ford and Milnes, 2008; Li et al., 2017), as this realistically occurs *in vivo* in the clinical setting. We only considered cardiotoxicity at the atrial level, assuming that the absence of I_{Kur} in ventricles prevents ventricular proarrhythmia. However, this might not be true for real I_{Kur} blockers with off-target effects. Here, we simulated I_{Kur} block at the cellular level with no contribution of structural tissue remodeling and defined I_{Kur} inhibitors' efficacy and toxicity by tracking only electrophysiological properties such as APD, ERP, CaT_{amp}, and diastolic $[Ca^{2+}]_i$. While this is an important first step in defining metrics for AF-selectivity, other arrhythmia indices and integration of such simulations into tissue and organ level models would improve our ability to discern best-performing drug characteristics of I_{Kur} inhibitors against AF. Since many antiarrhythmic drugs lose anti-AF efficacy with the progression of the arrhythmia, particularly in patients with atrial cardiomyopathy and comorbidities (Goette et al., 2016), I_{Kur} block might be less efficient against AF in the structurally remodeled atrium. Further studies including 2- and 3-dimensional tissue simulations are needed to address this clinically relevant issue. In addition, machine-learning methods have begun to be implemented to analyze AP metrics after the application of a drug and classify the risk (e.g., torsadogenic risk) of the candidate drug (Lancaster and Sobie, 2016). Such methods can also highlight which ion channels contribute most to such risk. Furthermore, this study revealed that the efficacy and toxicity of I_{Kur} inhibitors is modulated by the extent of atrial ionic remodeling, and likely by the relative expressions of many ion channels and transporters (Figures S1–S6). Thus, given the differences in AP properties and ion channel expression in patients with AF (Heijman et al., 2014), and differences in I_{Kur} remodeling in the right vs. the left atria (Dobrev and Ravens, 2003; Caballero et al., 2010), we hypothesize that certain subpopulations of nSR and cAF patients may be more responsive to therapy with I_{Kur} inhibitors, i.e., degree and heterogeneity of I_{Kur} remodeling in atrial tissue might impact safety and anti-AF efficacy of drugs. Future studies could identify which cell characteristics lead to more favorable responses to anti-I_{Kur} therapy utilizing sensitivity analysis and variations of nSR and cAF models similar to the methods discussed in **Figure 1** and in (Sobie, 2009; Lee et al., 2013; Cummins et al., 2014; Devenyi and Sobie, 2015; Morotti and Grandi, 2017). This information could be useful for a personalized (precision) medicine approach to AF treatment or helpful in suggesting potential combination therapies with I_{Kur} inhibitors.

Finally, advancements in high-throughput screening methods (Obergrussberger et al., 2016; Picones et al., 2016; Molokanova

et al., 2017) provide functional drug screening capabilities that can be coupled with *in silico* investigations such as the one described here to help identify actual candidate compounds for *in vivo* testing. Such technologies can potentially be implemented to simultaneously screen many $K_V1.5$-selective compounds for the desired kinetics, state-dependence, and rate-dependence of I_{Kur} block. In addition, multi-parallel recordings from atrial-like cardiomyocytes from induced human pluripotent stem cells is also emerging as a preclinical model for evaluating drugs targeting atrial-specific ion channels, such as $K_V1.5$ (Devalla et al., 2015), particularly in combination with AP-clamp experiments. These could be coupled with *in silico* studies such as this one for delineating the ideal properties of AF-selective drugs and gaining a more comprehensive understanding of the arrhythmic risk of candidate compounds.

CONCLUSIONS

In this study, efficacy and cardiotoxicity on cAF atrial cardiomyocytes of theoretical I_{Kur} inhibitors were assessed *in silico*. We concluded that I_{Kur} is a promising anti-AF target, even if strongly downregulated in cAF condition. We confirmed that steady-state IC_{50} values are insufficient to predict how candidate compounds will interact with a dynamically changing electrophysiological substrate, thus emphasizing the importance of accounting for kinetic and state-dependent drug-binding properties. This approach could aid experimental and screening efforts to identify the complex net impact of I_{Kur} inhibition in different AF-remodeling conditions during the pre-clinical drug development process.

AUTHOR CONTRIBUTIONS

Designed simulation experiments: NE, SM, EG. Performed modeling and simulations: NE, SM. Wrote the manuscript: NE, DD, SM, EG.

ACKNOWLEDGMENTS

The authors would like to thank Dr. Lucía Romero Pérez, Polytechnic University of Valencia, for her critical reading of this manuscript. This work was supported by the National Institute of Health grant R01-HL131517 (to EG and DD), the American Heart Association grant 15SDG24910015 (EG), the Heart Rhythm Society post-doctoral fellowship 16OA9HRS (SM), the Bill Bertken Sudden Death Prevention Fund, and the National Center for Advancing Translational Sciences, National Institutes of Health, through grant number UL1 TR001860 and linked award TL1 TR001861 (NE).

SUPPLEMENTARY MATERIAL

The Supplementary Material for this article can be found online at: https://www.frontiersin.org/articles/10.3389/fphar.2017.00799/full#supplementary-material

REFERENCES

Aguilar, M., Feng, J., Vigmond, E., Comtois, P., and Nattel, S. (2017). Rate-dependent role of I_{Kur} in human atrial repolarization and atrial fibrillation maintenance. *Biophys. J.* 112, 1997–2010. doi: 10.1016/j.bpj.2017.03.022

Amos, G. J., Wettwer, E., Metzger, F., Li, Q., Himmel, H. M., and Ravens, U. (1996). Differences between outward currents of human atrial, and subepicardial ventricular myocytes. *J. Physiol.* 491, 31–50. doi: 10.1113/jphysiol.1996.sp021194

Andrade, J., Khairy, P., Dobrev, D., and Nattel, S. (2014). The clinical profile and pathophysiology of atrial fibrillation: relationships among clinical features, epidemiology, and mechanisms. *Circ. Res.* 114, 1453–1468. doi: 10.1161/CIRCRESAHA.114.303211

Bers, D. M., and Grandi, E. (2011). Human atrial fibrillation: insights from computational electrophysiological models. *Trends Cardiovasc. Med.* 21, 145–150. doi: 10.1016/j.tcm.2012.04.004

Bosch, R. F., Zeng, X.,Grammer, J. B., Popovic, K., Mewis, C., and Kuhlkamp, V. (1999). Ionic mechanisms of electrical remodeling in human atrial fibrillation. *Cardiovasc. Res.* 44, 121–131. doi: 10.1016/S0008-6363(99)00178-9

Bouchard, R., and Fedida, D. (1995). Closed- and open-state binding of 4-aminopyridine to the cloned human potassium channel Kv1.5. *J. Pharmacol. Exp. Ther.* 275, 864–876.

Brandt, M. C., Priebe, L., Bohle, T., Sudkamp, M., and Beuckelmann, D. J. (2000). The ultrarapid and the transient outward K^+ current in human atrial fibrillation. Their possible role in postoperative atrial fibrillation. *J. Mol. Cell Cardiol.* 32, 1885–1896. doi: 10.1006/jmcc.2000.1221

Caballero, R., de la Fuente M. G., Gomez, R., Barana, A., Amoros, I., Dolz-Gaiton, P., et al. (2010). In humans, chronic atrial fibrillation decreases the transient outward current and ultrarapid component of the delayed rectifier current differentially on each atria and increases the slow component of the delayed rectifier current in both. *J. Am. Coll. Cardiol.* 55, 2346–2354. doi: 10.1016/j.jacc.2010.02.028

Cavero, I., and Holzgrefe, H. (2014). Comprehensive *in vitro* proarrhythmia assay, a novel *in vitro*/*in silico* paradigm to detect ventricular proarrhythmic liability: a visionary 21st century initiative. *Expert Opin. Drug Saf.* 13, 745–758. doi: 10.1517/14740338.2014.915311

Christ, T., Wettwer, E., Voigt, N., Hala, O., Radicke, S., Matschke, K., et al. (2008). Pathology-specific effects of the $I_{Kur}/I_{to}/I_{K,ACh}$ blocker AVE0118 on ion channels in human chronic atrial fibrillation. *Br. J. Pharmacol.* 154, 1619–1630. doi: 10.1038/bjp.2008.209

Christophersen, I. E., Olesen, M. S., Liang, B., Andersen, M. N., Larsen, A. P., Nielsen J. B., et al. (2013). Genetic variation in KCNA5: impact on the atrial-specific potassium current I_{Kur} in patients with lone atrial fibrillation. *Eur. Heart J.* 34, 1517–1525. doi: 10.1093/eurheartj/ehs442

Colman, M. A., Ni, H., Liang, B., Schmitt, N., and Zhang, H. (2017). *In silico* assessment of genetic variation in KCNA5 reveals multiple mechanisms of human atrial arrhythmogenesis. *PLoS Comput. Biol.* 13:e1005587. doi: 10.1371/journal.pcbi.1005587

Cummins, M. A., Dalal, P. J., Bugana, M., Severi, S., and Sobie, E. A. (2014). Comprehensive analyses of ventricular myocyte models identify targets exhibiting favorable rate dependence. *PLoS Comput. Biol.* 10:e1003543. doi: 10.1371/journal.pcbi.1003543

Devalla, H. D., Schwach, V., Ford, J. W., Milnes, J. T., El-Haou, S., Jackson C., et al. (2015). Atrial-like cardiomyocytes from human pluripotent stem cells are a robust preclinical model for assessing atrial-selective pharmacology. *EMBO Mol. Med* 7, 394–410. doi: 10.15252/emmm.201404757

Devenyi, R. A., and Sobie, E. A. (2015). There and back again: iterating between population-based modeling and experiments reveals surprising regulation of calcium transients in rat cardiac myocytes. *J. Mol. Cell Cardiol.* 96, 38–48. doi: 10.1016/j.yjmcc.2015.07.016

Dobrev, D., and Ravens, U. (2003). Remodeling of cardiomyocyte ion channels in human atrial fibrillation. *Basic Res. Cardiol.* 98, 137–148. doi: 10.1007/s00395-003-0409-8

Ehrlich, J. R., Biliczki, P., Hohnloser, S. H., and Nattel, S. (2008). Atrial-selective approaches for the treatment of atrial fibrillation. *J. Am. Coll. Cardiol.* 51, 787–792. doi: 10.1016/j.jacc.2007.08.067

Ellinwood, N., Dobrev, D., Morotti, S., and Grandi, E. (2017). Revealing kinetics and state-dependent binding properties of I_{Kur}-targeting drugs that maximize atrial fibrillation selectivity *Chaos* 27:093918. doi: 10.1063/1.5000226

Ford, J. W., and Milnes, J. T., (2008). New drugs targeting the cardiac ultra-rapid delayed-rectifier current I_{Kur}: rationale, pharmacology and evidence for potential therapeutic value. *J. Cardiovasc. Pharmacol.* 52, 105–120. doi: 10.1097/FJC.0b013e3181719b0c

Ford, J., Milnes, J., El Haou, S., Wettwer, E., Loose, S., Matschke, K., et al. (2016). The positive frequency-dependent electrophysiological effects of the I_{Kur} inhibitor XEN-D0103 are desirable for the treatment of atrial fibrillation. *Heart Rhythm* 13, 555–564. doi: 10.1016/j.hrthm.2015.10.003

Ford, J., Milnes, J., Wettwer, E., Christ, T., Rogers, M., Sutton, K., et al. (2013). Human electrophysiological and pharmacological properties of XEN-D0101: a novel atrial-selective Kv1.5/I_{Kur} inhibitor. *J. Cardiovasc. Pharmacol* 61, 408–415. doi: 10.1097/FJC.0b013e31828780eb

Goette, A., Kalman, J. M., Aguinaga, L., Akar, J., Cabrera, J. A., Chen S. A., et al. (2016). EHRA/HRS/APHRS/SOLAECE expert consensus on atrial cardiomyopathies: definition, characterization, and clinical implication. *Europace* 18, 1455–1490. doi: 10.1093/europace/euw161

Grammer, J. B., Bosch, R. F., Kuhlkamp, V., and Seipel, L. (2000). Molecular remodeling of Kv4.3 potassium channels in human atrial fibrillation. *J. Cardiovasc. Electrophysiol.* 11, 626–633. doi: 10.1111/j.1540-8167.2000.tb00024.x

Grandi, E., and Maleckar, M. M. (2016). Anti-arrhythmic strategies for atrial fibrillation: the role of computational modeling in discovery, development, and optimization. *Pharmacol. Ther.* 168, 126–142. doi: 10.1016/j.pharmthera.2016.09.012

Grandi, E., Pandit, S. V., Voigt, N., Workman, A. J., Dobrev, D., Jalife, J., et al. (2011). Human atrial action potential and Ca^{2+} model: sinus rhythm and chronic atrial fibrillation. *Circ. Res.* 109, 1055–1066. doi: 10.1161/CIRCRESAHA.111.253955

Grandi, E., Workman, A. J., and Pandit, S. V. (2012). Altered excitation-contraction coupling in human chronic atrial fibrillation. *J. Atr. Fibrillation* 4:495. doi: 10.4022/jafib.495

Heijman, J., Voigt, N., Nattel, S., and Dobrev, D. (2014). Cellular and molecular electrophysiology of atrial fibrillation initiation, maintenance, and progression. *Circ. Res.* 114, 1483–1499. doi: 10.1161/CIRCRESAHA.114.302226

Lagrutta, A., Wang, J., Fermini, B., and Salata, J. J. (2006). Novel, potent inhibitors of human Kv1.5 K^+ channels and ultrarapidly activating delayed rectifier potassium current. *J. Pharmacol. Exp. Ther.* 317, 1054–1063. doi: 10.1124/jpet.106.101162

Lancaster, M. C., and Sobie, E. A. (2016). Improved prediction of drug-induced torsades de pointes through simulations of dynamics and machine learning algorithms. *Clin. Pharmacol. Ther.* 100, 371–379. doi: 10.1002/cpt.367

Lee, W., Mann, S. A., Windley,M. J., Imtiaz, M. S., Vandenberg, J. I., and Hill, A. P. (2016). *In silico* assessment of kinetics and state dependent binding properties of drugs causing acquired LQTS. *Prog. Biophys. Mol. Biol.* 120, 89–99. doi: 10.1016/j.pbiomolbio.2015.12.005

Lee, Y. S., Liu, O. Z., Hwang, H. S., Knollmann, B. C. and Sobie, E. A. (2013). Parameter sensitivity analysis of stochastic models provides insights into cardiac calcium sparks. *Biophys. J.* 104, 1142–1150. doi: 10.1016/j.bpj.2012.12.055

Li, Z., Dutta, S., Sheng, J., Tran, P. N., Wu, W., Chang, K. et al. (2017). Improving the *In silico* assessment of proarrhythmia risk by combining hERG (human ether-a-go-go-related gene) channel-drug binding kinetics and multichannel pharmacology. *Circ. Arrhythm. Electrophysiol.* 10:e004628. doi: 10.1161/CIRCEP.116.004628

Loose, S., Mueller, J., Wettwer, E., Knaut, M., Ford, J., Milnes, J., et al. (2014). Effects of I_{Kur} blocker MK-0448 on human right atrial action potentials from patients in sinus rhythm and in permanent atrial fibrillation. *Front. Pharmacol.* 5:26. doi: 10.3389/fphar.2014.00026

Molokanova, E., Mercola, M., and Savchenko, A. (2017). Bringing new dimensions to drug discovery screening: impact of cellular stimulation technologies. *Drug Discov. Today* 22, 1045–1055. doi: 10.1016/j.drudis.2017.01.015

Morotti, S., and Grandi, E. (2017). Logistic regression analysis of populations of electrophysiological models to assess proarrythmic risk. *MethodsX* 4, 25–34. doi: 10.1016/j.mex.2016.12.002

Morotti, S., Koivumäki, J. T., Maleckar, M. M., Chiamvimonvat, N., and Grandi, E. (2016a). Small-conductance Ca^{2+}-activated K^+ current in atrial fibrillation: both friend and foe. *Biophys. J.* 110:274a. doi: 10.1016/j.bpj.2015.11.1487

Morotti, S., McCulloch, A. D., Bers, D. M., Edwards, A. G., and Grandi, E. (2016b). Atrial-selective targeting of arrhythmogenic phase-3 early afterdepolarizations in human myocytes. *J. Mol. Cell Cardiol.* 96, 63–71. doi: 10.1016/j.yjmcc.2015.07.030

Morotti, S., Nieves-Cintron, M., Nystoriak, M. A., Navedo, M. F., and Grandi, E. (2017). Predominant contribution of L-type Cav1.2 channel stimulation to impaired intracellular calcium and cerebral artery vasoconstriction in diabetic hyperglycemia, *Channels* 11, 340–346. doi: 10.1080/19336950.2017.1293220

Nattel, S., and Dobrev, D. (2016). Electrophysiological and molecular mechanisms of paroxysmal atrial fibrillation. *Nat. Rev. Cardiol.* 13, 575–590. doi: 10.1038/nrcardio.2016.118

Obergrussberger, A., Bruggemann, A., Goetze, T. A., Rapedius, M., Haarmann, C., Rinke, I., et al. (2016). Automated patch clamp meets high-throughput screening: 384 cells recorded in parallel on a planar patch clamp module. *J. Lab. Autom.* 21, 779–793. doi: 10.1177/2211068215623209

Olson, T. M., Alekseev, A. E., Liu, X. K., Park, S., Zingman, L.V., Bienengraeber, M., et al. (2006). Kv1.5 channelopathy due to KCNA5 loss-of-function mutation causes human atrial fibrillation. *Hum. Mol. Genet.* 15, 2185–2191. doi: 10.1093/hmg/ddl143

Picones, A., Loza-Huerta, A., Segura-Chama, P., and Lara-Figueroa, C. O. (2016). Contribution of automated technologies to ion channel drug discovery. *Adv. Protein Chem. Struct. Biol.* 104, 357–378. doi: 10.1016/bs.apcsb.2016.01.002

Ravens, U., Poulet, C., Wettwer, E., and Knaut, M. (2013). Atrial selectivity of antiarrhythmic drugs *J. Physiol.* 591, 4087–4097. doi: 10.1113/jphysiol.2013.256115

Sanchez, C., Corrias, A., Bueno-Orovio, A., Davies, M., Swinton, J., Jacobson, I., et al. (2012). The Na^+/K^+ pump is an important modulator of refractoriness and rotor dynamics in human atrial tissue. *Am. J. Physiol. Heart Circ. Physiol.* 302, H1146–H1159. doi: 10.1152/ajpheart.00668.2011

Schotten, U., de Haan, S., Verheule, S., Harks, E. G., Frechen, D. Bodewig, E., et al. (2007). Blockade of atrial-specific K^+-currents increases atrial but not ventricular contractility by enhancing reverse mode Na^+/Ca^{2+}-exchange. *Cardiovasc. Res.* 73, 37–47. doi: 10.1016/j.cardiores.2006.11.024

Shinagawa, K., Mitamura, H., Takeshita, A., Sato, T., Kanki, H., Takatsuki, S., et al. (2000). Determination of refractory periods and conduction velocity during atrial fibrillation using atrial capture in dogs: direct assessment of the wavelength and its modulation by a sodium channel blocker, pilsicainide. *J. Am. Coll. Cardiol.* 35, 246–253. doi: 10.1016/S0735-1097(99)00488-X

Sobie, E. A. (2009). Parameter sensitivity analysis in electrophysiological models using multivariable regression. *Biophys. J.* 96, 1264–1274. doi: 10.1016/j.bpj.2008.10.056

Tsujimae, K., Murakami, S., and Kurachi, Y. (2008). *In silico* study on the effects of I_{Kur} block kinetics on prolongation of human action potential after atrial fibrillation-induced electrical remodeling. *Am. J. Physiol. Heart Circ. Physiol.* 294, H793–H800. doi: 10.1152/ajpheart.01229.2007

Van Wagoner, D. R., and Nerbonne, J. M. (2000). Molecular basis of electrical remodeling in atrial fibrillation. *J. Mol. Cell Cardiol.* 32, 1101–1117. doi: 10.1006/jmcc.2000.1147

Van Wagoner, D. R., Piccini, J. P., Albert, C. M., ,Anderson, M. E., Benjamin, E. J., Brundel, B. et al. (2015). Progress toward the prevention and treatment of atrial fibrillation: a summary of the heart rhythm society research forum on the treatment and prevention of atrial fibrillation, Washington, DC, December 9–10, 2013. *Heart Rhythm* 12, e5–e29. doi: 10.1016/j.hrthm.2014.11.011

Van Wagoner, D. R., Pond, A. L., McCarthy, P. M., Trimmer, J. S., and Nerbonne, J. M. (1997). Outward K^+ current densities and $K_v1.5$ expression are reduced in chronic human atrial fibrillation. *Circ. Res.* 80, 772–781. doi: 10.1161/01.RES.80.6.772

Wang, D., Shryock, J. C., and Belardinelli, L. (1996). Cellular basis for the negative dromotropic effect of adenosine on rabbit single atrioventricular nodal cells. *Circ. Res.* 78, 697–706. doi: 10.1161/01.RES.78.4.697

Wettwer, E., Hala, O., Christ, T., Heubach, J. F., Dobrev, D., Knaut, M., et al. (2004). Role of I_{Kur} in controlling action potential shape and contractility in the human atrium: influence of chronic atrial fibrillation. *Circulation* 110, 2299–2306. doi: 10.1161/01.CIR.0000145155.60288.71

Workman, A. J., Kane, K. A., and Rankin, A. C. (2001). The contribution of ionic currents to changes in refractoriness of human atrial myocytes associated with chronic atrial fibrillation. *Cardiovasc. Res.* 52, 226–235. doi: 10.1016/S0008-6363(01)00380-7

Yue, L., Feng, J., Gaspo, R., Li, G. R., Wang, Z., and Nattel, S. (1997). Ionic remodeling underlying action potential changes in a canine model of atrial fibrillation. *Circ. Res.* 81, 512–525. doi: 10.1161/01.RES.81.4.512

Zhao, Q., Tang, Y., Okello, E., Wang, X., and Huang, C. (2009). Changes in atrial effective refractory period and I_{KACh} after vagal stimulation plus rapid pacing in the pulmonary vein. *Rev. Esp. Cardiol* 62, 742–749. doi: 10.1016/S0300-8932(09)71687-2

Zhou, Q., Bett, G. C., and Rasmusson, R. L. (2012). Markov models of use-dependence and reverse use-dependence during the mouse cardiac action potential. *PLoS ONE* 7:e42295. doi: 10.1371/journal.pone.0042295

Conflict of Interest Statement: The authors declare that the research was conducted in the absence of any commercial or financial relationships that could be construed as a potential conflict of interest.